Iron deposition and fat accumulation in dimethylnitrosamine-induced liver fibrosis in rat

Jin-Yang He, Wen-Hua Ge, Yuan Chen

Jin-Yang He, Tropical Medicine Institute of Guangzhou University of Chinese Medicine, Guangzhou 510405, Guangdong Province, China
Wen-Hua Ge, Department of Warm Diseases of Guangzhou University of Chinese Medicine, Guangzhou 510405, Guangdong Province, China
Yuan Chen, Humanities and Social Sciences Faculty of Guangzhou University of Chinese Medicine, Guangzhou, 510405, Guangdong Province, China
Correspondence to: Dr. Jin-Yang He, Tropical Medicine Institute of Guangzhou University of Chinese Medicine, Guangzhou 510405, Guangdong Province, China. sunny12345678_89@yahoo.com.cn
Telephone: +86-20-31774402 Fax: +86-20-86575767
Received: 2006-12-15   Accepted: 2007-02-13

Abstract

AIM: To investigate if iron deposition and fat accumulation in the liver play a pathogenetic role in dimethylnitrosamine (DMN)-induced liver fibrosis in rat.

METHODS: Thirty rats were treated with DMN at does consecutive days of 10 μL/kg daily, i.p., for 3 consecutive day each week for 4 wk. Rats ($n = 30$) were sacrificed on the first day (model group A) and 21st d (model group B) after cessation of DMN injection. The control group ($n = 10$) received an equivalent amount of saline. Liver tissues were stained with hematoxylin & eosin (HE) and Masson and Prussian blue assay and oberserved under electron microscopy. Serum alanine aminotransferase (ALT) and liver tissue hydroxyproline (Hyp) content were tested.

RESULTS: The liver fibrosis did not automatically reverse, which was similar to previous reports, the perilobular deposition of iron accompanied with collagen showed marked characteristics at both the first and 21st d after cessation of DMN injection. However, fat accumulation in hepatocytes occurred only at the 21st d after cessation of DMN injection.

CONCLUSION: Iron deposition and fat accumulation may play important roles in pathological changes in DMN-induced rat liver fibrosis. The detailed mechanisms of these characteristics need further research.

He JY, Ge WH, Chen Y. Iron deposition and fat accumulation in dimethylnitrosamine-induced liver fibrosis in rat. *World J*

INTRODUCTION

Iron deposition and liver steatosis are important pathological changes in chronic liver diseases like viral hepatitis and alcoholic liver diseases[1-5]. The two pathological changes have also been demonstrated to occur in CCL$_4$-induced liver damage or fibrosis[6,7]. Iron overload in the liver may damage hepatocyte and stimulate reactive oxygen species and lipid peroxidation, eventually resulting in liver fibrosis, cirrhosis, or other liver diseases[8-10]. Additionally, liver steatosis is also closely related to fibrosis and can increase the severity of fibrosis[11]. It was reported that hepatic inflammation may mediate fibrogenesis in patients with liver steatosis[12].

Rat liver fibrosis induced by dimethylnitrosamine (DMN) is a good reproducible model and has been widely used in screening drugs and researching mechanisms associated with liver fibrosis or cirrhosis[13-16]. However, it is currently unknown whether iron deposition and fat accumulation also occur in DMN-induced rat liver fibrosis.

The pathogenesis of this model includes fibrillar septa formation, focal nodule formation, biochemical abnormalities and the development of ascites[13,14]. After cessation of DMN, the death of rats continued and liver function continues to deteriorate over time[17]. Anti-fibrotic drugs usually need to be administered for as long as about 3 wk to evaluate their effects. Therefore, this study determined the characteristics of the time points at the first day and 21st d after cessation of DMN.

MATERIALS AND METHODS

Animals
Male and female Sprague-Dawley rats of 120-150 g body weight were used. They were fed with standard rat diet and water according to guidelines approved by the China Association of Laboratory Animal Care. They were settled in plastic cages in an SPF-grade animal room in the Experimental Animal Center of Guangzhou University of Chinese Medicine.

Treatment protocol
The rats were randomly divided into the control group

Figure 1 Schematic representation of the DMN treatment protocol.

Table 1 Changes of serum ALT and tissue Hyp means ± SD

Group	n	ALT (U/mL)	Hyp (μg/g)
Control	10	20.8 ± 4.96	109.14 ± 29.06
Model A	10	60.2 ± 8.01[b]	351.46 ± 65.86[b]
Model B	12	58 ± 10.32[a,b]	367.37 ± 42.06[a,b]

Statistical method: Nemenyi method. [a]$P > 0.05$ *vs* model A; [b]$P < 0.01$ *vs* Control.

and the model group. The animals in the model group (n = 30) received DMN (Tianjin Chemical Reagent Research Institute) dissolved in saline at does of 10 μL DMN/kg, i.p., for 3 consecutive d each wk for 4 wk. The control group (n = 10) received an equivalent amount of saline. On the last day of DMN administration, the rats in model group were randomly divided into 2 groups as group model A and group model B. Group model A (n = 10) rats were sacrificed on the first d after cessation of DMN and group B and the control group were sacrificed in 21st d after cessation of DMN. The treatment protocol is presented in Figure 1.

Histopathology

The liver tissue was observed under light microscopy after fixation with Bouin fluid for 24-36 h. Paraffin sections were stained with hematoxylin & eosin (HE) for routine examination, followed by Masson staining for collagen, and Prussian blue for iron. Processing for electron microscopy included fixation with glutaraldehyde in 0.2 mol/L phosphate buffer and embedding in epon/araldite.

Quantitative determination of the deposition of collagen, fat and iron

Quantitative determination of collagen was done by analyzing the Masson-stained paraffin sections under an optical microscope by a grading method. The degree of fibrosis of liver sections was graded numerically based on the following criteria: 0, no fibrosis; + 1, slight fibrosis, fibrosis located in the central liver lobule; + 2, moderate fibrosis, widened central fibrosis; + 3, severe fibrosis, fibrosis extended to the edge of liver lobule; + 4, liver cirrhosis.

A grading method through analyzing the sections under electron microscopy was used for quantitative evaluation of fat accumulation according to previous methods[18]. The four-point scale was: 0-4 or none, normal, slight, moderate and severe. Scores 1-4 are considered to correspond to fat deposition in 5%-10% 10%-33%, 33%-66% and > 66% of the hepatocytes, respectively; 0 represents < 5% of the hepatocytes.

The semiquantitative measurement of iron deposition was done using the following criteria: the blue-colored iron particles were divided into 4 sizes as small (graded as 1), middle (2), large (3), or larger (4). Three closely linked lobules and their perilobular spaces of each Prussian blue-stained section were randomly chosen to count the iron particles and analyze the size for calculating iron deposition scores.

Biochemical measurements

The serum alanine aminotransferase (ALT) levels were measured using an ultraviolet method. The liver tissue

hydroxyproline (Hyp) content was determined according to the method of Sakaida *et al*[14].

Statistical analysis

Results are expressed as means ± SD. Nemenyi's method or Student's *t* test were used to determine comparisons between two groups. BiomedCalc software was used for statistical analysis.

RESULTS

Grossly observed changes

Throughout the experiments, the body weight of most treated animals increased regularly but remained 30% lower than the weight of controls, except for 3 treated animals, who did not show an increase in weight. The animals started to die from the 4th wk of treatment and continued to the last d of cessation of observation. In total, 8 rats died during the whole observation period, 1 died before the cessation of DMN and 7 died after the cessation of DMN. Upon opening of the abdomen, the liver of all treated animals showed diffuse hyperemia and granularity in the liver surface. Ascites were visible in all treated rats. Three bloody ascites were found in treated rats sacrificed at the first day after cessation of DMN. The other treated rats had bloody acites when sacrificed at the last d of observation.

Serum ALT levels and liver tissue Hyp

Both the serum ALT and liver tissue Hyp were markedly increased at the first day after cessation of DMN (model A). By the 21st d (model B) after cessation of DMN, the serum ALT and liver tissue Hyp were also markedly increased and were not significantly different compared with the 1st d after cessation of DMN. The level of serum ALT and liver tissue Hyp are shown in Table 1.

Histopathological manifestatiion

The liver lobules of the control group showed no pathological changes and the liver cells were normal (Figure 2A).There were pseudo-lobules in 8 samples at the first d after cessation of DMN). Large numbers of black and brown particles were deposited and accompanied with fibrosis tissue (Figure 2B). A similar pattern was evident in model B, with pseudo-lobules present in 9 samples. Hemorrhagic necrosis and mononuclear infiltration was slight but there was still evidence of new bleeding in all the samples with HE staining. Compared with model A, liver cell steatosis was apparent in 7 of 12 samples in model B (Figure 2C). Each sample of models A and B showed enlarged portal tracts and severe fibrosis deposition (Figure
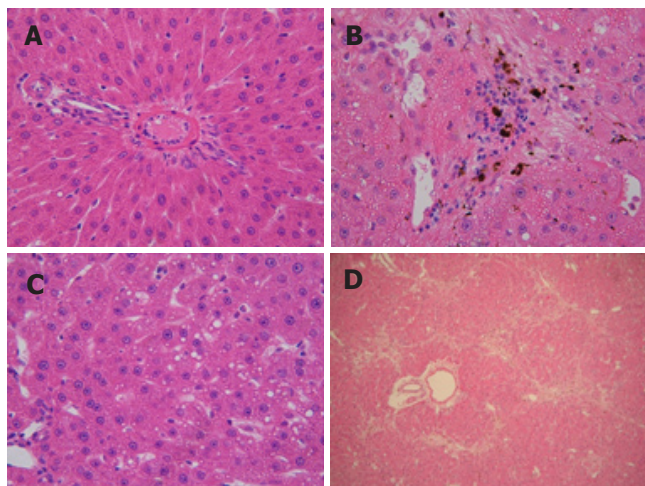
Figure 2 Liver histopathology of DMN-treated rats (HE). **A**: Control group, no marked pathological changes (× 400); **B**: Group model A, hemorrhagic necrosis with foci of lymphomonocytic infiltration around fibrosis tissue can be seen (× 400); **C**: Group model B, fat accumulated in numerous liver cells (× 400); **D**: Group model B, quantities of fiber deposited and linked with each other (× 400).
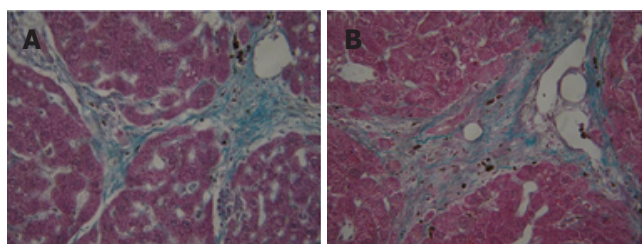
Figure 3 Rat liver fibrosis induced by DMN (Masson). **A**: Group model A, the green fiber distributed between liver cells and accompanied with necrotic hemorrhage; **B**: Group model B, similar to group model A in fibrosis (× 400).

2D). Hemorrhagic necrosis with foci of lymphomonocytic infiltration around fibrosis tissue can be seen.

The collagen was shown to be green-colored in the Masson-stained section. The collagen was mainly deposited perilobularly without marked differences in location or severity of collagen deposition between the first (Figure 3A) and 21st d (Figuire 3B) after cessation of DMN.

Electron microscopy showed that in the first day after cessation of DMN, there were alterations of sinusoidal walls accompanied with numerous erythrocytes in the space of Disse and some of the erythrocytes nearly touched the liver cell membrane (Figure 4A). Other structural alterations of liver cells included altered mitochondrial configuration and evidence of intracellular bile retention with a distorted canalicular membrane. Numerous transitional cells showing the features of lipid-containing myofibroblases were observed although there was no fat accumulation in liver cells in all the samples of the group. However, on the 21st d after cessation of DMN, numerous liver cells containing small or large fat droplets were found in all the samples of the group (Figure 4B). Extended segments of the sinusoidal wall were still deprived of endothelium. Myofibroblasts and typical fibroblasts were numerous in fibrotic septa. Occasional plasma cells were also observed together with lymphoid
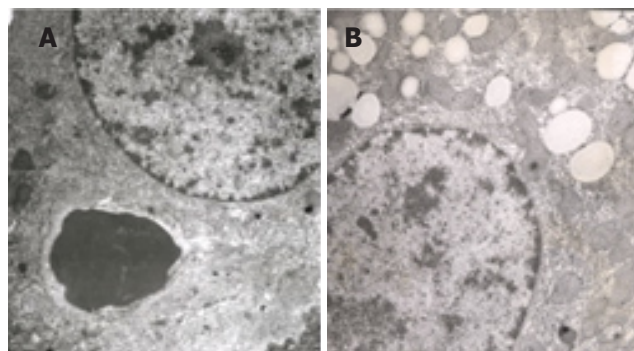
Figure 4 Ultrastructural changes of the liver in DMN-treated rats. **A**: model group A, no marked lipid drops deposited in the liver cells and from which we also can see an erythrocyte pass through extracellular matrix and closely stick to the liver cell membrane; **B**: model group B, numerous lipid drops deposited in liver cell (electron microscopy, × 6000).
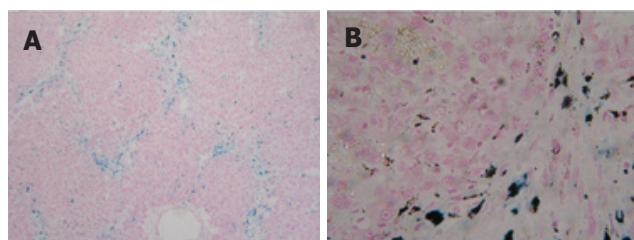
Figure 5 Iron deposition in rat liver induced by DMN (Prussian blue). **A**: model group **A**, the iron is mainly accompanied by fiber (× 100); **B**: model group B, similar to the model A in iron deposition, iron nodules are deep blue in color and mainly located extracellularly or in the Kupffer cells (× 400).

Table 2 Histopathological semiquantitative scores of collagen deposition in the liver

Groups	*n*	0	+1	+2	+3	+4	Staging scores (mean ± SD)
Control	10	10	0	0	0	0	0
Model A	10	0	0	1	1	8	3.70 ± 0.67
Model B	12	0	0	1	2	9	3.67 ± 0.65[a]

Statistic method: Student's *t* test. [a]$P > 0.05$ *vs* model B.

cells in close contact with hepatocytes.

Prussian blue-stained sections showed that the black and brown particles in the HE-stained sections were iron particles (Figure 5A and B). The iron was mainly deposited around liver lobules. Few hepatocytes showed invasion by iron and most of the iron was extracellularly deposited or in the kupffer cells.

Semiquantitative measurement of collagen, fat and iron

The results showed that the collagen deposition scores (Table 2) are markedly increased on both the first and 21st d after cessation of DMN compared with the control group, although there were no marked differences between the two time points ($P > 0.05$). However, fat accumulation (Table 3) was significantly increased on the 21st d ($P < 0.01$) after cessation of DMN, but not on the first day ($P > 0.05$). Similar to the collagen deposition, iron deposition

Table 3 Histopathological semiquantitative scores of fat deposition in the liver

Groups	n	0	+1	+2	+3	+4	Staging scores (mean ± SD)
Control	3	1	2	0	0	0	0.67 ± 0.58
Model A	3	1	2	0	0	0	0.67 ± 0.58[a]
Model B	3	0	0	0	2	1	3.33 ± 0.58[b]

Statistic method: Student's t test. [b]P < 0.01 vs control group; [a]P > 0.05 vs control group.

Table 4 Histopathological semiquantitative scores of iron deposition in the liver

Groups	n	Iron deposition scores (mean ± SD)
Control	10	0
Model A	10	396.10 ± 32.83
Model B	12	389.92 ± 49.42[a]

Statistic method: Student's t test. [a]P > 0.05 vs model B.

(Table 4) was markedly increased in both of the model groups compared with control group, but there were no differences between the two model groups.

DISCUSSION

In the present study special attention was paid to the time points of the first and 21st d after cessation of DMN injection, which is closely associated with liver fibrosis reversal during drug screening. DMN was injected for 3 consecutive days each week for 4 wk, which is a similar modeling method for drug screening. The results showed that serum ALT, liver tissue Hyp and liver collagen staging scores showed no significant differences between the first d and 21st d after cessation of DMN. These results revealed that the severity of liver fibrosis was not significantly reversed after cessation of DMN for 3 wk. Additionally, this model has the following merits: (1) as a good reproducible model, fewer rats died during the whole observation stage and a shorter time was spent for modeling compared with CCL$_4$-induced rat liver fibrosis, (2) the mechanism of DMN-induced liver fibrosis has been shown to be associated with immune function, which is similar to the mechanism of human liver fibrosis[19]. Thus, DMN-induced rat liver fibrosis may be a useful model for determination of liver fibrosis during drug screening.

The tissue pathological changes of DMN-induced rat liver fibrosis are reported to include fibrillar septa formation, focal nodule formation and severe hemorrhage. A three-week treatment with a low dose of DMN produces micronodular cirrhosis following diffuse hemorrhagic necrosis without steatosis (35th d of observation, 19 d after cessation of treatment)[20]. In a longer duration study[20], liver steatosis was not found after cessation of DMN for 24 wk. However, in the present study, liver cell steatosis was observed in 7 of 12 samples of Model B with HE stain on the 45th d of observation (4 wk DMN administration and 21 d of treatment cessation). Under electron microscope, numerous liver cells containing small or large fat droplets were found in all the samples at the 21st d after cessation of DMN. But in the model group A, there was no marked deposition of fat drops, which was similar to the control group in liver cells in all of the samples both with HE staining and under the electron microscope. This experiment was repeated twice and similar results were obtained. This phenomenon revealed that treatment with DMN for 3 consecutive days each weak for 4 wk can result in significantly different liver tissue pathological changes compared with 3 wk or other time spans of DMN treatment.

According to recent studies, steatosis is involved in liver pathological changes[11], and it has also been demonstrated that steatosis is a cofactor of other liver diseases[5]. Steatosis of both alcohol and nonalcoholic-related etiologies is associated with the development of more advanced diseases, including necroinflammation (steatohepatitis), fibrosis, and cirrhosis[21]. There is also direct evidence showing a correlation between the severity of steatosis and the degree of hepatic stellate cell activation[22]. Steatosis of most nonalcoholic etiologies is also associated with the development of necroinflammation (so-called non-alcoholic steatohepatitis or NASH)[21]. There are also studies demonstrating that steatosis is a direct contributor to inflammation and/or fibrosis[23,24]. In the present study, the accumulation of fat drops in liver cells occurred only in model group B (21st d after cessation of DMN treatment), suggesting that although DMN treatment was stopped, lipid metabolism had been perturbed by necroinflammation or fibrosis. On the contrary, the lipid deposition may exacerbate fibrosis and/or inflammation.

Previous studies have not discussed the role of iron deposition in DMN-induced rat liver fibrosis. In this study, we showed that the iron deposition accompanied with fibrosis and increased numbers of erythrocytes in the liver tissue is a marked phenomenon in both models A and B. This may indicate that the deposited iron may play a role in the maintenance and progression of pathological changes in the liver after cessation of DMN treatment. Additionally, the iron is mainly extracellularly deposited or in Kupffer cells and is accompanied with fiber, which may block the nutrition and information transfer between cells or lobes. The hemorrhage in liver fibrosis is severe and the iron in the erythrocytes situated near the normal liver cells can be metabolized. However, when the cell function of fibrotic tissue is attenuated, the Kupffer cells and liver cells are not capable of processing the iron in the erythrocytes located close to the fiber and, consequently, the iron is deposited. Adversely, the deposited iron can accelerate the advancement of liver fibrosis and may even facilitate hepatocarcinogenesis[25,26]. Is this a general principle of liver diseases typified with chronic hemorrhage? This may need further research. Actually, Iron deposition is characteristics of many forms of liver diseases including viral hepatitis B[27], C[28], alcoholic[29] and nonalcoholic[30,31] hepatitis. In the experimental animal model, Iron overload can enhance the development of CCL$_4$-induced liver cirrhosis of mice[32]. Iron toxicity may thus be due to promotion of

oxidant stress. It has been reported that free radicals and membrane oxidation by-products can cause hepatocellular death by triggering organelle dysfunction, or by activating cells involved in hepatic inflammation and fibrogenesis, such as Kupffer cells and hepatic stellate cells[33]. Actually, iron deposition characterizes many forms of DMN-induced rat liver fibrosis.

REFERENCES

1   **Purohit V**, Russo D, Salin M. Role of iron in alcoholic liver disease: introduction and summary of the symposium. *Alcohol* 2003; **30**: 93-97

2   **Thorburn D**, Curry G, Spooner R, Spence E, Oien K, Halls D, Fox R, McCruden EA, MacSween RN, Mills PR. The role of iron and haemochromatosis gene mutations in the progression of liver disease in chronic hepatitis C. *Gut* 2002; **50**: 248-252

3   **Tung BY**, Emond MJ, Bronner MP, Raaka SD, Cotler SJ, Kowdley KV. Hepatitis C, iron status, and disease severity: relationship with HFE mutations. *Gastroenterology* 2003; **124**: 318-326

4   **Erhardt A**, Maschner-Olberg A, Mellenthin C, Kappert G, Adams O, Donner A, Willers R, Niederau C, Häussinger D. HFE mutations and chronic hepatitis C: H63D and C282Y heterozygosity are independent risk factors for liver fibrosis and cirrhosis. *J Hepatol* 2003; **38**: 335-342

5   **Powell EE**, Jonsson JR, Clouston AD. Steatosis: co-factor in other Liver diseases. *Hepatology* 2005; **42**: 5-13

6   **López A**, Carmona CA, Moussatche H. On the mechanism of protective action of cold acclimatization against carbon tetrachloride- and ethionine-induced fatty liver. *Mem Inst Oswaldo Cruz* 1993; **88**: 313-316

7   **Batey RG**, Johnston R. Effects of alcohol, carbon tetrachloride, and choline deficiency on iron metabolism in the rat. *Alcohol Clin Exp Res* 1993; **17**: 931-934

8   **Khan MF**, Wu X, Tipnis UR, Ansari GA, Boor PJ. Protein adducts of malondialdehyde and 4-hydroxynonenal in livers of iron loaded rats: quantitation and localization. *Toxicology* 2002; **173**: 193-201

9   **Svegliati-Baroni G**, Saccomanno S, van Goor H, Jansen P, Benedetti A, Moshage H. Involvement of reactive oxygen species and nitric oxide radicals in activation and proliferation of rat hepatic stellate cells. *Liver* 2001; **21**: 1-12

10   **Wang GS**, Eriksson LC, Xia L, Olsson J, Stål P. Dietary iron overload inhibits carbon tetrachloride-induced promotion in chemical hepatocarcinogenesis: effects on cell proliferation, apoptosis, and antioxidation. *J Hepatol* 1999; **30**: 689-698

11   **Day CP**, James OF. Hepatic steatosis: innocent bystander or guilty party? *Hepatology* 1998; **27**: 1463-1466

12   **Leandro G**, Mangia A, Hui J, Fabris P, Rubbia-Brandt L, Colloredo G, Adinolfi LE, Asselah T, Jonsson JR, Smedile A, Terrault N, Pazienza V, Giordani MT, Giostra E, Sonzogni A, Ruggiero G, Marcellin P, Powell EE, George J, Negro F. Relationship between steatosis, inflammation, and fibrosis in chronic hepatitis C: a meta-analysis of individual patient data. *Gastroenterology* 2006; **130**: 1636-1642

13   **Yen MH**, Weng TC, Liu SY, Chai CY, Lin CC. The hepatoprotective effect of Bupleurum kaoi, an endemic plant to Taiwan, against dimethylnitrosamine-induced hepatic fibrosis in rats. *Biol Pharm Bull* 2005; **28**: 442-448

14   **Sakaida I**, Hironaka K, Terai S, Okita K. Gadolinium chloride reverses dimethylnitrosamine (DMN)-induced rat liver fibrosis with increased matrix metalloproteinases (MMPs) of Kupffer cells. *Life Sci* 2003; **72**: 943-959

15   **Hu QW**, Liu GT. Effects of bicyclol on dimethylnitrosamine-induced liver fibrosis in mice and its mechanism of action. *Life Sci* 2006; **79**: 606-612

16   **George J**. Mineral metabolism in dimethylnitrosamine-induced hepatic fibrosis. *Clin Biochem* 2006; **39**: 984-991

17   **Jenkins SA**, Grandison A, Baxter JN, Day DW, Taylor I, Shields R. A dimethylnitrosamine-induced model of cirrhosis and portal hypertension in the rat. *J Hepatol* 1985; **1**: 489-499

18   **Franzén LE**, Ekstedt M, Kechagias S, Bodin L. Semiquantitative evaluation overestimates the degree of steatosis in liver biopsies: a comparison to stereological point counting. *Mod Pathol* 2005; **18**: 912-916

19   **Jézéquel AM**, Mancini R, Rinaldesi ML, Ballardini G, Fallani M, Bianchi F, Orlandi F. Dimethylnitrosamine-induced cirrhosis. Evidence for an immunological mechanism. *J Hepatol* 1989; **8**: 42-52

20   **Jézéquel AM**, Mancini R, Rinaldesi ML, Macarri G, Venturini C, Orlandi F. A morphological study of the early stages of hepatic fibrosis induced by low doses of dimethylnitrosamine in the rat. *J Hepatol* 1987; **5**: 174-181

21   **Bacon BR**, Farahvash MJ, Janney CG, Neuschwander-Tetri BA. Nonalcoholic steatohepatitis: an expanded clinical entity. *Gastroenterology* 1994; **107**: 1103-1109

22   **Reeves HL**, Burt AD, Wood S, Day CP. Hepatic stellate cell activation occurs in the absence of hepatitis in alcoholic liver disease and correlates with the severity of steatosis. *J Hepatol* 1996; **25**: 677-683

23   **Lieber CS**. Alcohol and the liver: 1994 update. *Gastroenterology* 1994; **106**: 1085-1105

24   **Diehl AM**, Goodman Z, Ishak KG. Alcohollike liver disease in nonalcoholics. A clinical and histologic comparison with alcohol-induced liver injury. *Gastroenterology* 1988; **95**: 1056-1062

25   **Mueller S**, Afdhal NH, Schuppan D. Iron, HCV, and liver cancer: hard metal setting the pace? *Gastroenterology* 2006; **130**: 2229-2234

26   **Ioannou GN**, Kowdley KV. Iron, HFE mutations, and hepatocellular carcinoma: is hepatic iron a carcinogen? *Clin Gastroenterol Hepatol* 2003; **1**: 246-248

27   **Chrobot A**, Chrobot AM, Szaflarska-Szczepanik A. Assessment of iron metabolism in children with chronic hepatitis B -- prognostic factor in interferon alpha therapy. *Med Sci Monit* 2002; **8**: CR269-CR273

28   **Sebastiani G**, Vario A, Ferrari A, Pistis R, Noventa F, Alberti A. Hepatic iron, liver steatosis and viral genotypes in patients with chronic hepatitis C. *J Viral Hepat* 2006; **13**: 199-205

29   **Kohgo Y**, Ohtake T, Ikuta K, Suzuki Y, Hosoki Y, Saito H, Kato J. Iron accumulation in alcoholic liver diseases. *Alcohol Clin Exp Res* 2005; **29**: 189S-193S

30   **Fierbinţeanu-Braticevici C**, Bengus A, Neamţu M, Usvat R. The risk factors of fibrosis in nonalcoholic steatohepatitis. *Rom J Intern Med* 2002; **40**: 81-88

31   **Bugianesi E**, Manzini P, D'Antico S, Vanni E, Longo F, Leone N, Massarenti P, Piga A, Marchesini G, Rizzetto M. Relative contribution of iron burden, HFE mutations, and insulin resistance to fibrosis in nonalcoholic fatty liver. *Hepatology* 2004; **39**: 179-187

32   **Arezzini B**, Lunghi B, Lungarella G, Gardi C. Iron overload enhances the development of experimental liver cirrhosis in mice. *Int J Biochem Cell Biol* 2003; **35**: 486-495

33   **Corradini E**, Ferrara F, Pietrangelo A. Iron and the liver. *Pediatr Endocrinol Rev* 2004; **2** Suppl 2: 245-248